Marine and Petroleum Geology xxx (2014) 1–13

Contents lists available at ScienceDirect

Marine and Petroleum Geology

journal homepage: www.elsevier.com/locate/marpetgeo

Sedimentation rates from calcareous nannofossil and planktonic foraminifera biostratigraphy in the Andaman Sea, northern Bay of Bengal, and eastern Arabian Sea

J.A. Flores [a, *], J.E. Johnson [b], A.E. Mejía-Molina [a], M.C. Álvarez [a], F.J. Sierro [a], S.D. Singh [c], Syamal Mahanti [c], L. Giosan [d]

[a] Grupo de Geociencias Oceanicas, Departamento de Geología, Universidad de Salamanca, Salamanca 37008, Spain
[b] Department of Earth Sciences, University of New Hampshire, Durham, NH 03824, USA
[c] Oil and Natural Gas Corporation Ltd. (ONGC), Dehradun 248195, India
[d] Department of Geology and Geophysics, Woods Hole Oceanographic Institute, Woods Hole, MA 02543, USA

ARTICLE INFO

Article history:
Received 2 March 2014
Received in revised form
13 August 2014
Accepted 14 August 2014
Available online xxx

Keywords:
Indian Ocean
Calcareous plankton biochronology
NGHP-01
Age model
Hiatuses

ABSTRACT

In this study we determined calcareous nannofossil and planktonic foraminifera events in sediments recovered during the 2006 Indian National Gas Hydrate Program (NGHP) Expedition-01. Selected bioevents permitted the assignment of orbitally calibrated ages, derivative sedimentation rate estimates, and identification of sedimentary discontinuities. In the Andaman Sea at Hole NGHP-01-17A, a late Miocene to recent record was recovered, but with a significant hiatus during the latest Miocene and Pliocene. Sedimentation rates here vary from 50 m/Myr during the Pleistocene to 130 m/Myr for the late Miocene. In the northern Bay of Bengal at Hole NGHP-01-19A the base of the cored record also reaches the late Miocene and extends to recent, but the same hiatus, missing the Pliocene, is present at this hole. a. The Early Pleistocene at Hole NGHP-1-19A shows sensible variation in sedimentation rates ranging between 130 m/Myr and 10 m/Myr during the last 0.5 Ma. For the late Miocene the sedimentation rate was ca. 50 m/Myr. In the western Bay of Bengal at Hole NGHP-01-10B/D, calcareous nannofossils were sparse and only foraminifera datums are available. The base of the section is latest Early Pliocene to Late Pliocene, and the majority of the record is considered younger than Late Pliocene. Due to the scarcity of calcareous nannofossils and the few foraminifera datums, sedimentation rates were not determined here. However, Hole NGHP-01-16A, in the same region, recorded the highest occurrence of *Pseudoemiliania lacunosa*, an event that confirms a Pleistocene age, allowing us to estimate a sedimentation rate between 110 m/Myr and 450 m/Myr. Along the western peninsular Indian margin at Hole NGHP-01-01A a continuous record from the Holocene to the early Oligocene indicates sedimentation rates of ca. 25 m/Myr until the middle Miocene, and a sensible reduction downward, reaching 4 m/Myr in the early Miocene to the early Oligocene. No hiatuses were observed. The large changes in sedimentation rates observed in these cores reflect long timescale changes in the environment likely induced by changes in the strength of the Indian monsoon system.

1. Introduction

The slope environments in the Andaman Sea, northern Bay of Bengal, and eastern Arabian Sea margins are located in oceanic regions where continental margin sediments accumulate in response to tectonic and climate forcing. There are few scientific ocean drilling expeditions (DSDP, ODP, IODP) in these regions (Fig. 1), however, limiting our understanding of sediment accumulation patterns on million year timescales in these environments. In 2006 the Indian National Gas Hydrate Program (NGHP) carried out its first drilling and coring expedition in Indian territorial waters (Collett et al., 2008), recovering cores in the Bay of Bengal from 17 sites in the offshore Krishna–Godavari Basin, 2 sites in the offshore Mahanadi Basin, and 1 site in the accretionary wedge of the Sunda subduction zone in the Andaman Sea (Fig. 1). In addition, one site was cored in the Kerala–Konkan basin on the western peninsular Indian margin in the Arabian Sea (Fig. 1). The

* Corresponding author.
E-mail address: flores@usal.es (J.A. Flores).

http://dx.doi.org/10.1016/j.marpetgeo.2014.08.011
0264-8172/

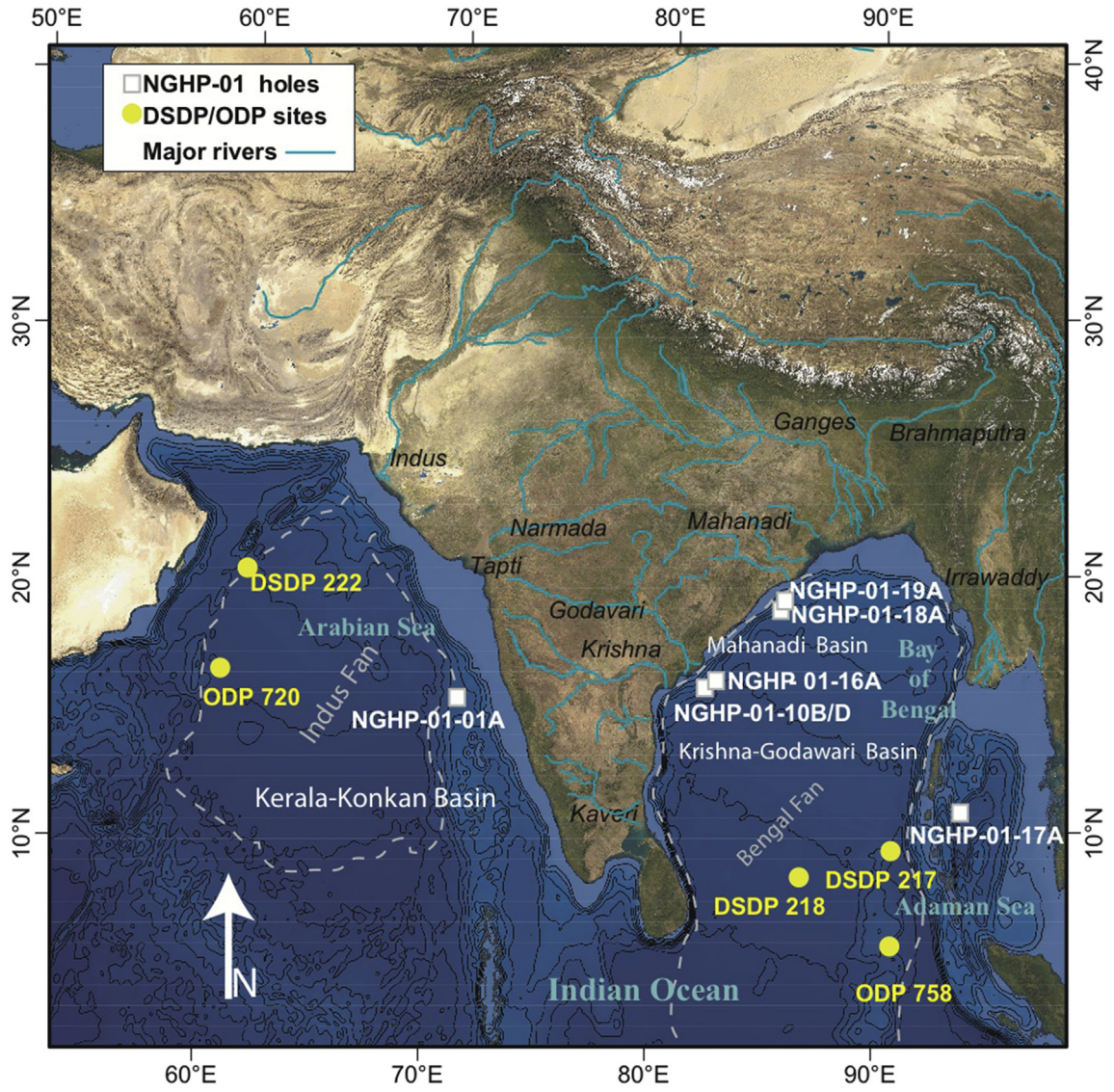

Figure 1. Site location map with the NGHP-01 holes examined in this study plus the existing DSDP and ODP sites in the region. The dotted line marks the Indus and Bengal fans.

sedimentary records on the eastern peninsular margin of India are located in sedimentary basins (Krishna–Godavari and Mahanadi) in the slope environment above the Bengal Fan depositional system (Fig. 1). These sites are also located in close proximity to the peninsular Indian Krishna, Godavari, and Mahanadi Rivers, which deliver significant lithogenic sedimentary materials to these core sites across a narrow continental shelf (Collett et al., 2008; Phillips et al., 2014a,b; Johnson et al., 2014), diluting the biogenic sedimentary constituents. The core site on the western peninsular margin of India is located on the continental slope, above the Indus fan depositional system, and far from the minor rivers that drain western peninsular India (Fig. 1). The record here is dominated by biogenic carbonate oozes (Collett et al., 2008) with less contribution from terrestrial lithogenic or carbon sources (Phillips et al., 2014a; Johnson et al., 2014). The core site in the Andaman accretionary wedge is located above both the Bengal–Nicobar Fan depositional system and the Andaman back-arc basin (Fig. 1). The sedimentary record here is dominated by carbonate oozes and biosiliceous carbonate oozes punctuated by airfall volcanic ashes (Collett et al., 2008; Cawthern et al., 2014; Rose et al., 2014). Clay mineralogy is dominated by smectite throughout the record, and most likely sourced from local volcanic ash sources (Phillips et al., 2014a,b).

In this paper we provide a first attempt at age-models for these records at a resolution significant enough to interpret variations in patterns of sedimentation and the continuity of the records in these regions. Here we present calcareous nannofossil and planktonic foraminifera biostratigraphy from at least one core in each of the four study regions. The identification of calcareous nannofossil and planktonic foraminifer orbitally calibrated events (e.g. Lourens et al., 2004; Raffi et al., 2006; Wade et al., 2011) have been then used to calculate sedimentation rates, which are important for understanding terrigenous and biogenic sedimentary fluxes, linked to regional geological and climatic processes. These age models have been used initially to interpret longer timescale variations in productivity (Cawthern et al., 2014), carbon sources and abundance (Johnson et al., 2014), and lithogenic fluxes (Phillips et al., 2014a,b) in these regions and serve to guide future scientific drilling expeditions and biostratigraphic studies to help constrain the history and evolution of the Indian monsoon.

Please cite this article in press as: Flores, J.A., et al., Sedimentation rates from calcareous nannofossil and planktonic foraminifera biostratigraphy in the Andaman Sea, northern Bay of Bengal, and eastern Arabian Sea, Marine and Petroleum Geology (2014), http://dx.doi.org/10.1016/j.marpetgeo.2014.08.011

2. Geological setting and lithology

The Bay of Bengal in the northern Indian Ocean is dominated by the Bengal and Nicobar submarine fan systems, which have received terrigenous sediments from the erosion of the Himalayan Mountains and transport through the Ganges–Brahmaputra drainage systems during the last 15 million years (Curray et al., 2003; Bastia et al., 2010) (Fig. 1). The extent of the Bengal Fan is limited to the west by the continental shelf and slope of peninsular India, which formed as a passive margin during the break-up of Gondwana (Powell et al., 1988; Ramana et al., 2001; Radhakrishna et al., 2012) and has received terrigenous sediments from the modern Mahanadi, Krishna, Godavari, and Kaveri Rivers and predecessor rivers (Fig. 1). Holes NGHP-01-10B/D, NGHP-01-16A, and NGHP-01-18A and NGHP-01-19A, are all located on the slope, above the modern-day depocenter of the Bengal Fan, on the eastern margin of peninsular India, near the mouth of the Krishna and Godavari rivers and south of the Mahanadi River discharge, respectively (Fig. 1). The sediments deposited in the offshore K–G basin are sourced from the Krishna and Godavari Rivers, which drain the Deccan Basalts and deliver suspended sediment loads rich in smectite with minor feldspar, quartz, kaolinite, and illite (Subramanian, 1980; Phillips et al., 2014b) to the offshore margin. Sediments deposited in the offshore Mahanadi basin are sourced from the two regions: the eastern Deccan drained by the Mahanadi River and the Precambrian Eastern Ghat province (Rickers et al., 2001; Phillips et al., 2014b). Illite is the dominant clay mineral in the Mahanadi basin, followed by kaolinite, smectite, and chlorite and quartz, feldspar, and dolomite are characteristic in suspended sediments discharged by the Mahanadi to the Bay of Bengal (Chakrapani and Subramanian, 1990; Subramanian, 1980; Phillips et al., 2014b). The Hole NGHP-01-10B/D and NGHP-01-16A preserve a terrigenous dominated record of silty clay with silt and sand turbidites, while Hole NGHP-01-18A and Hole NGHP-01-19A records consists of silty clay composed of a mixture of biogenic and lithogenic materials (Collett et al., 2008; Phillips et al., 2014a). Hole NGHP-01-10B/D is located in a water depth of 1049.4 m, Hole NGHP-01-16A in 1253 m, Hole NGHP-01-18A in 1374 m, and Hole NGHP-01-19A in 1422 m.

In the eastern Bay of Bengal, the Bengal Fan has been subducted or accreted beneath the Sunda Subduction Zone (Bowles et al., 1978; Curray et al., 2003). Farther to the east, the semi-enclosed Andaman Sea is located in a back-arc basin formed by the oblique subduction of the Indian Plate beneath the Sunda Plate (Rodolfo, 1969; Karig et al., 1980; Pal et al., 2003; Raju et al., 2007). Within the Andaman Sea, terrigenous sediments from the Irrawaddy River are deposited on the shelf and slope, north of the Andaman back-arc spreading center (Ramaswamy et al., 2008). Transportation of fine-grained sediments from the modern Irrawaddy is restricted to the nearshore region by monsoonal surface currents (Rodolfo, 1975; Babu et al., 2010; Tripathy et al., 2011). Hole NGHP-01-17A is located in the Andaman accretionary wedge, east of Little Andaman Island and contains a record of carbonate and siliceous oozes punctuated by volcanic ash deposits (Collett et al., 2008; Cawthern et al., 2014; Rose et al., 2014). The clay mineralogy is dominated by smectite (Phillips et al., 2014b) and Hole NGHP-01-17A is located in a water depth of 1336 m (Table 1).

The western continental margin of India formed during the break-up of the Gondwana supercontinent during the Mesozoic (Kalaswad et al., 1993; Royer et al., 2002). The large sediment flux associated with erosion of the Himalayas and Tibetan Plateau and transport to the Arabia Sea via the Indus river results in the development the Indus fan (Clift et al., 2001), the second largest submarine fan on Earth. The Chagos–Laccadive Ridge is a prominent N–S trending aseismic ridge offshore western India that most likely represents a hotspot track that evolved from past spreading ridge and Reunion hotspot volcanism (Duncan and Pyle, 1988; Fisk et al., 1989). Western peninsular India has a well-defined escarpment, the Western Ghats or Sahyadri, running parallel the coast for 1500 km at an average height of 1200 m (Campanile et al., 2008). The Western Ghats form the drainage divide for peninsular India and Ramaswamy et al. (1991) show that almost all of the river discharge from western peninsular India is retained on the shelf. Hole NHGP-01-1A is located nearly on line with the Chagos–Laccadive Ridge, just north of where it disappears as a bathymetric feature and contains a sedimentary record of predominantly carbonate oozes (Collett et al., 2008). Clay mineralogy at this hole is dominated by illite and the bulk mineralogy by calcite (Phillips et al., 2014b). Hole NGHP-01-01A is located in a water depth of 2674.2 m (Table 1).

Table 1
Location of the sites studied.

Hole	Position	Depth (mbsf[a])	Region
NGHP-01-1A	15° 18.366′N, 070° 54.192′E	2674.2	Arabian Sea Kerala–Konkan Basin
NGHP-01-17A	10° 45.1912′N, 93° 6.7365′E	1336	Eastern Bay of Bengal Andaman Sea
NGHP-01-10B/D	15° 51.8609′N, 81° 50.0749′E	1049.4	Western Bay of Bengal Krishna–Godavari Basin
NGHP-01-16A	16° 35.5986′N, 082° 41.007′E	1253.0	Western Bay of Bengal Krishna–Godavari Basin
NGHP-01-18A	19° 09.1452′N, 85° 46.3758′E	1374.0	North Western Bay of Bengal Mahanadi Basin
NGHP-01-19A	18° 58.6568′N, 85° 39.5202′E	1422.0	North Western Bay of Bengal Mahanadi Basin

[a] mbsf = meters below seafloor.

3. Materials and methods

3.1. Calcareous nannofossils

A total of 313 samples were studied in the four NGHP-01 study regions (130 for Hole NGHP-01-1A, 71 for Hole NGHP-01-17A, 30 for Hole NGHP-01-10D, 22 for Hole NGHP-01-16A, 20 for Hole NGHP-01-18A and 71 for Hole NGHP-01-19A). Sampling was carried out in equidistant intervals of ~9 m in order to sample the record uniformly and to detect significant chronostratigraphically calibrated bioevents and/or characteristics of standard zonal schemes. Smear slides were prepared from unprocessed sediment and were examined with a polarizing microscope (Leica DMRP) at ×1000 magnification. Occasionally, ×1250 and ×1600 magnification was also used for the identification of very small specimens as well as characteristics related to the preservation of calcareous nannofossils. For this study, only biostratigraphically significant taxa or morphotypes are considered. A general view of the rest of the assemblage was also considered for supporting environmental compatibility of the markers, as well as for estimation of the state of preservation. Around 3 mm^2 (ca. 200 visual fields at ×1000) were examined to estimate semi-quantitative abundance. Additionally, two to three additional traverses of slides were scanned to detect the presence of rare or very rare specimens. These abundance patterns were considered to define the lowest and highest occurrences (LO and HO). Preservation of nannoliths was estimated following Flores and Marino (2002). In general, except in marked intervals barren in calcareous nannofossils, preservation is good to

Please cite this article in press as: Flores, J.A., et al., Sedimentation rates from calcareous nannofossil and planktonic foraminifera biostratigraphy in the Andaman Sea, northern Bay of Bengal, and eastern Arabian Sea, Marine and Petroleum Geology (2014), http://dx.doi.org/10.1016/j.marpetgeo.2014.08.011

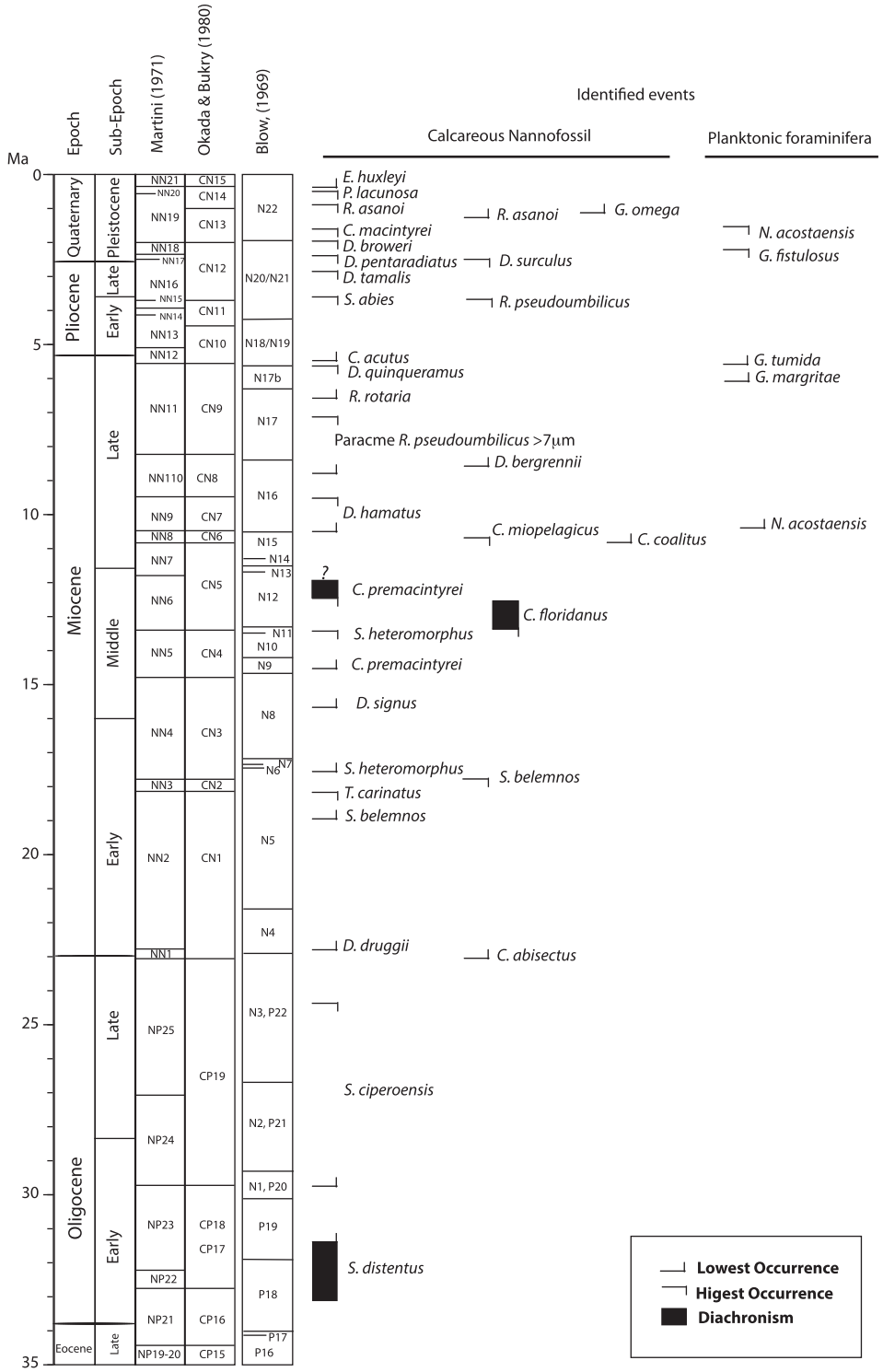

Figure 2. Calcareous nannofossils and planktonic foraminifera standard zonation and the chronostratigraphic context of the events used in this study.

moderate, allowing the identification of most of the specimens. The intervals barren in calcareous nannofossils are delimited and detailed in the next section.

3.2. Planktonic foraminifera

Samples for the study of planktonic foraminifera were soaked in a mixture of dilute hydrogen peroxide and ammonia solution for up to six hours and boiled in sodium carbonate for nearly ten minutes. Disaggregated material was subjected to ultrasonic treatment for up to thirty seconds and sieved through a 300 mesh screen. The material >300 mesh fraction was dried in an oven at 50 °C. The processed material was then dry sieved through a 150 mesh screen and the fractions were archived separately. Foraminifera were studied under a NIKON Stereoscopic Zoom Microscope SMZ1500. Bioevents of stratigraphically lowest and highest occurrences (LO and HO) were identified throughout the records. A total of 70 samples were examined for foraminiferal studies in three of the

Table 2
Assignation of ages ATNTS04 (Astronomical Tuned Neogene Time Scale; Gradstein et al., 2004) to calcareous nannofossil and planktonic foraminifera bioevents identified in the NGHP studied sites.

Calcareous nannofossils event	Age (Ma)	Planktonic foraminifers event	Age (Ma)	Reference	Holes (mbsf)					
					1A	19A	18A	17A	16A	10B/D
LO *E. huxleyi*	0.29			Raffi et al. (2006)	1.5	14.98	26.83		31.35	
HO *P. lacunosa*	0.44			Raffi et al. (2006)	18.98	63.99	115.91	36.36	219.2	
HO *R. asanoi*	0.9			Raffi et al. (2006)						
LO *Gephyrocapsa* sp. 3	1.01			Raffi et al. (2006)	27.8					
LO *R. asanoi*	1.14			Raffi et al. (2006)				80.72		
HO *C. macintyrei*	1.6			Raffi et al. (2006)	32.55			109.43		
		HO *N. acostaensis*	1.58	Lourens et al. (2004)						186.83
		HO *G. fistulosus*	1.88	Wade et al. (2011)				99.3		
HO *D. broweri*	2.06			Raffi et al. (2006)	48.8	75.44				
HO *D. pentaradiatus*	2.39			Raffi et al. (2006)	58.3					
HO *D. surculus*	2.52			Raffi et al. (2006)	63.05			118.9		
HO *D. tamalis*	2.87			Raffi et al. (2006)	63.05			165.62		
HO *Sphenolithus* spp.	3.65			Raffi et al. (2006)	72.55	89.19		165.62		
HO *Reticulofenestra* >7 μm	3.79			Raffi et al. (2006)	77.3	89.19		165.62		
LO *C. acutus*	5.32			Raffi et al. (2006)	103.5					
		LO *G. Tumida*	5.51	Wade et al. (2011)		138				
HO *D. quinqueramus*	5.59			Raffi et al. (2006)	107.8	187.13		185.22		
HO *R. rotaria*					121.3					
		LO *G. margaritae*	5.95	Wade et al. (2011)				326.2		
LO *R. rotaria*	6.68			6.50 Ma recalibrated Raffi and Flores (1995)	129.8			241.59		
Top paracme *Reticulofenestra* >7 μm	7.08			Raffi et al. (2006)	137.3	243.89		346.5		
LO *D. surculus*	7.88				170.1					
LO *D. berggreni*	8.52			Raffi et al. (2006)	152.63			502.65		
Bottom paracme *Reticulofenestra* >7 μm	8.78			Raffi et al. (2006)	164.15			644.36		
HO *D. hamatus*	9.56			Raffi et al. (2006)	170.1			676.85		
		LO *N. acostaensis*	9.79	Wade et al. (2011)		213.6		496		
LO *D. hamatus*	10.54			Raffi et al. (2006)	176.4					
LO *C. coalitus*	10.78			Raffi et al. (2006)	178.4					
HO *C. miopelagicus*	10.63			Raffi et al. (2006)	184.3					
LO *C. nitescens*	12.25			Raffi et al. (2006)	188.43					
HO *C. premacintyrei*	12.47				187.8					
HO *S. heteromorphus*	13.53			Raffi et al. (2006)	194.9					
HO *C. floridanus*	12.03				205.8					
LO *D. sgnus*	15.7			Raffi et al. (2006)	—					
LO *C. premacintyrei*	14.67			14.70 Ma recalibrated Berggren et al. (1995)	—					
LO *S. heteromorphus*	17.72			Raffi et al. (2006)	219.1					
HO *S. belemnos*	17.97			Raffi et al. (2006)	215.4					
HO *T. carinatus*	18.31			Raffi et al. (2006)	226.6					
LO *S. belemnos*	18.92			Raffi et al. (2006)	226.6					
LO *D. druggi*	22.82			Lourens et al. (2004)	237.7					
LO *T. carinatus*				Without calibration	258.38					
LO *C. abisectus*				Without calibration	243.5					
HO *S. ciperoensis*	24.24			Raffi et al. (1995)	251.6					
LO *S. ciperoensis*	29.9			Berggren et al. (1995)	266.65					
LO *S. distentus*	31.5—33.1			Berggren et al. (1995)	266.65					
HO *H. compacta*				Without calibration	271.15					

HO = highest occurrence.
LO = lowest occurrence.

four NGHP-01 study regions (20 samples from Holes NGHP-01-10B and NGHP-01-10D, 34 samples from Holes NGHP-01-17A and 16 samples from Hole NGHP-01-19A) (Fig. 1).

4. Results and discussion

For this study selected bioevents were considered and adopted to define a nannofossil biostratigraphic pattern using the standard marker taxa (when preserved) shown in Martini (1971) and using the Okada and Bukry (1980) biozonation schemes. Selected bioevents were considered from Perch-Nielsen (1985), Olafsson (1989), Fornaciari et al. (1990, 1993, 1996), Rio et al. (1990a,b), Bukry (1991), Gartner (1992), Raffi and Flores (1995), Raffi et al. (1995), Fornaciari and Rio (1996), De Kaenel and Villa (1996), Bown and Young (1998), Maiorano and Monechi (1998), Marino and Flores (2002a,b), among others. Additionally, biochronology was developed following Backman, and Shackleton, 1983, Raffi and Flores (1995), Lourens et al. (2004) and Raffi et al. (2006), using astronomically calibrated ages from magnetic reversals and reference isotope stratigraphies, adjusted to the ATNTS2004 (Astronomical Tuned Neogene Time Scale; Gradstein et al., 2004). For planktonic foraminifera the calibration of Lourens et al. (2004) together with the review by Wade et al. (2011), are used. Figure 2 and Table 2 show the chronostratigraphic, events related to standard biozones (Blow, 1969 – as amended by Kennett and Srinivasan, 1983 –, Martini, 1971; Okada and Bukry, 1980) and supplementary events with calibrated datums. Below we describe the biostratigraphic constraints and the age models and

Please cite this article in press as: Flores, J.A., et al., Sedimentation rates from calcareous nannofossil and planktonic foraminifera biostratigraphy in the Andaman Sea, northern Bay of Bengal, and eastern Arabian Sea, Marine and Petroleum Geology (2014), http://dx.doi.org/10.1016/j.marpetgeo.2014.08.011

subsequent sedimentation rate estimates in each of the four study regions.

4.1. Hole NGHP-01-1A

4.1.1. Pleistocene–Holocene

Hole NGHP-01-01A was cored to 290 m. Standard calcareous nannofossil markers (Martini, 1971; Okada and Bukry, 1980) were only occasionally identified in this interval. Consequently, the strict adoption of these schemes is limited. However, the use of alternative bioevents (as mentioned above) permits the correlation of biozones, as is shown in Figure 3 and Table 2. The latest Pleistocene, and potentially the Holocene, is identified in the upper portion of the core at 1.5 mbsf. The absence of *Pseudoemiliania lacunosa* at 18.98 mbsf, approximates the limit of the late Pleistocene. Specimens close to the morphology of *Reticulofenestra asanoi* are present in an interval around 30 mbsf, but its size is smaller than 6 μm and its morphology is intermediate with *P. lacunosa*. Sato and Takayama (1992) defined this taxon considering individuals larger than 6 μm, thus we discard events (HO and LO) related to this species. Alternatively, the regular record of *Gephyrocapsa omega* (medium sized specimens; Raffi et al., 2006) is observed above 27.80 mbsf. The HO of *Calcidiscus macintyrei* is placed at 32.55 mbsf. *Discoaster bruweri* (HO) is last observed at 48.80 mbsf, whereas the HO of *Discoaster pentaradiatus* is placed at 58.30 mbsf. The number of discoasters in this hole is restricted, limiting the identification of conventional zonal boundaries (Fig. 2).

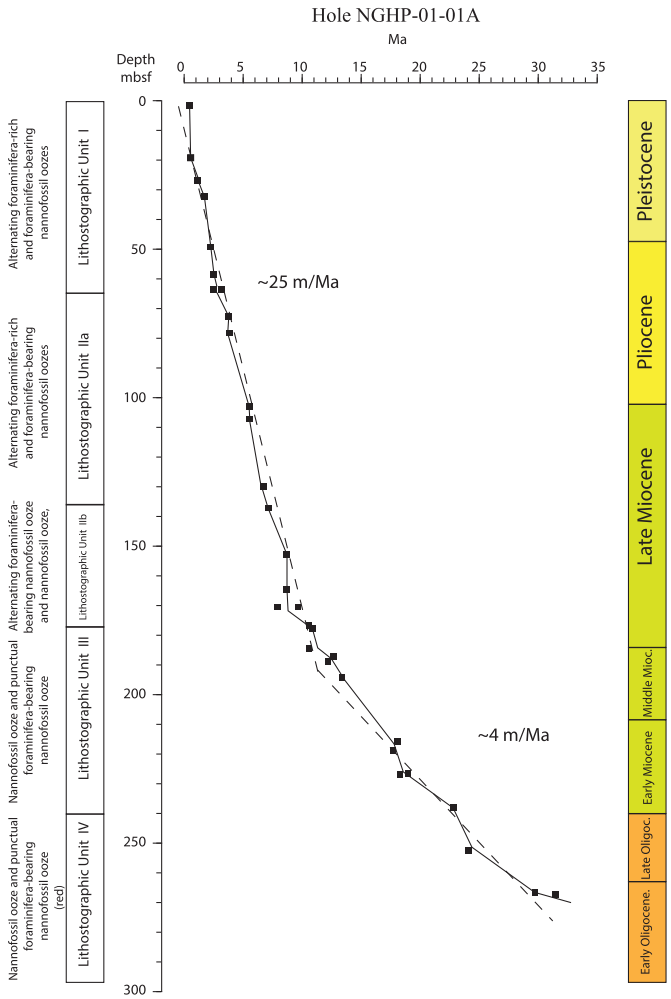

Figure 3. Distribution of calcareous nannofossil and planktonic foraminifera events vs. age according to ATNTS04 (Astronomical Tuned Neogene Time Scale; Gradstein et al., 2004) scale for Hole NGHP-01-01A. The small black squares represent calcareous nannofossil events (Table 1).

4.1.2. Pliocene

Discoaster surculus and *Discoaster tamalis* (HOs) below 63.05 mbsf is the closest event to the Pliocene/Pleistocene boundary, although the mentioned HO of *D. pentaradiatus* could be equally used. Other late Pliocene events are the HO of *Sphenolithus abies* and the HO of *Reticulofenestra pseudoumbilicus*; these taxa are frequent below 72.55 mbsf and 77.30 mbsf, respectively. The LO of *Ceratholithus acutus* is placed at 103.50 mbsf, characterizing the early Pliocene, and close to the Pliocene/Miocene boundary in absence of *Discoaster quinqueramus* in the underlying portion. Ceratoliths and triquetrorhabdoliths, the most used calcareous nannofossils in this interval, are scarce preventing a better biochronological pattern.

4.1.3. Miocene

Circular specimens assigned to *Reticulofenestra rotaria*, were observed above 129.80 mbsf. The HO of this species is not easy to define because of the presence of intermediate specimens with other medium-sized reticulofenestrids, although tentatively it is approximate to 121.30 mbsf. Raffi and Flores (1995) used the term "circular reticulofenestrids" for this taxon, and dated its LO and HO in the equatorial pacific; these same events are recalibrated in this work to the ATNTS2004 as show in Table 2.

The so-called paracme of *R. pseudoumbilicus* (>7 μm), interval where specimens of this species show sizes below this measure, is a worldwide event characteristic from the late Miocene, and here the LO is defined up to 164.15 mbsf. At 152.63 mbsf is recorded the LO of *Discoaster berggrenii*, inside the mentioned paracme (e.g. Raffi and Flores, 1995; Raffi et al., 2006). Occasional specimens of *R. pseudoumbilicus* (>7 μm) were recorded after this event. Those individuals are interpreted as reworked and, therefore, prevent the precise identification of the paracme's HO, which nonetheless is tentatively placed at 137.30 mbsf.

The early Miocene is characterized by the presence (LO + HO) of *Discoaster hamatus* identified between 176.45 and 170.1 mbsf. The LO of *Catinaster coalitus* occurs at 178.7 mbsf, whereas the HO of *Coccolithus miopelagus* is identified at 184.3 mbsf. Close to these events, at 187.8 mbsf was placed the HO of *Calcidiscus premacintyrei*. The highest consistent occurrence (Raffi et al., 2006) of this event is mentioned after the HO of *Calcidiscus miopelagicus*, interpreting that in this hole the event is not equivalent to that, because according with these authors was occasionally recorded in minor proportions later (here is not considered for biochronological considerations). Around this depth is identified the LO of *Triquetrorhabdulus rioi*, useful to determine the middle Miocene (Bown and Young, 1998), but not well calibrated yet. Specimens of *Cyclicargolithus floridanus* are regularly observed downwards 205.80 mbsf. Bioevents related to this taxon are defined quantitatively (e.g. the highest consistent occurrence, Raffi et al., 2006) and are not feasible for this study where only semi-quantitative data were produced, explaining the diachronism shown in Figure 2.

The HO and LO of *Sphenolithus heteromorphus* are identified at 194.9 mbsf and 219.1 mbsf, respectively. The sporadic presence of *Discoaster signus* and *C. premacintyrei* at the base of the middle Miocene, prevents final identification of their FO at this hole, although are present. The HO of *Sphenolithus belemnos* is recorded at 215.4 mbsf, and the LO at 226.6 mbsf, at the same depth that the HO of *Triquetrorhabdulus carinatus*. These events characterize the upper part of the early Miocene. The regular record (LO) of *Discoaster druggi* is identified at 237.7 mbsf, at the base of the early Miocene.

Please cite this article in press as: Flores, J.A., et al., Sedimentation rates from calcareous nannofossil and planktonic foraminifera biostratigraphy in the Andaman Sea, northern Bay of Bengal, and eastern Arabian Sea, Marine and Petroleum Geology (2014), http://dx.doi.org/10.1016/j.marpetgeo.2014.08.011

The HO of *Cyclicargolithus abisectus* at 243.5 mbsf approximates the Miocene–Oligocene boundary. The HO and LO of *Sphenolithus ciperoensis* is identified between 266.6 mbsf and 251.6 mbsf, respectively. The last event approximate the upper part of the early Oligocene, at the same time that the HO of *Sphenolithus distentus*, a markedly diachronous event (Berggren et al., 1995). The lowest event identified is the HO of *Helicosphaera compacta* used to approximate the middle–late Oligocene, at around 30 Ma (Bown and Young, 1998), although this age is not still well calibrated. Planktonic foraminifers were not examined at this hole.

4.1.4. Estimation of sedimentation rate

This hole shows a continuous record of sedimentation from the Holocene to the early Oligocene, permitting the identification of most of the standard biozonations (Fig. 2). The LO of *S. ciperoensis* at 266.65 mbsf allows to estimate an age close to 25 Ma for this horizon.

The sedimentation rate is around 25 m/Myr from the top to the middle early Miocene. From this depth to the base of the record, there is a decrease of the sedimentation rate, showing a mean value of 4 m/Myr (Fig. 3). The apparent synchronicity of different events is related to the low sampling resolution.

4.2. Hole NGHP-01-17A

Hole NGHP-01-17A shows a more irregular biostratigraphic succession, with intervals where preservation is moderate, and the abundance of calcareous nannofossil is variable. Data are shown in Figure 4 and Table 2.

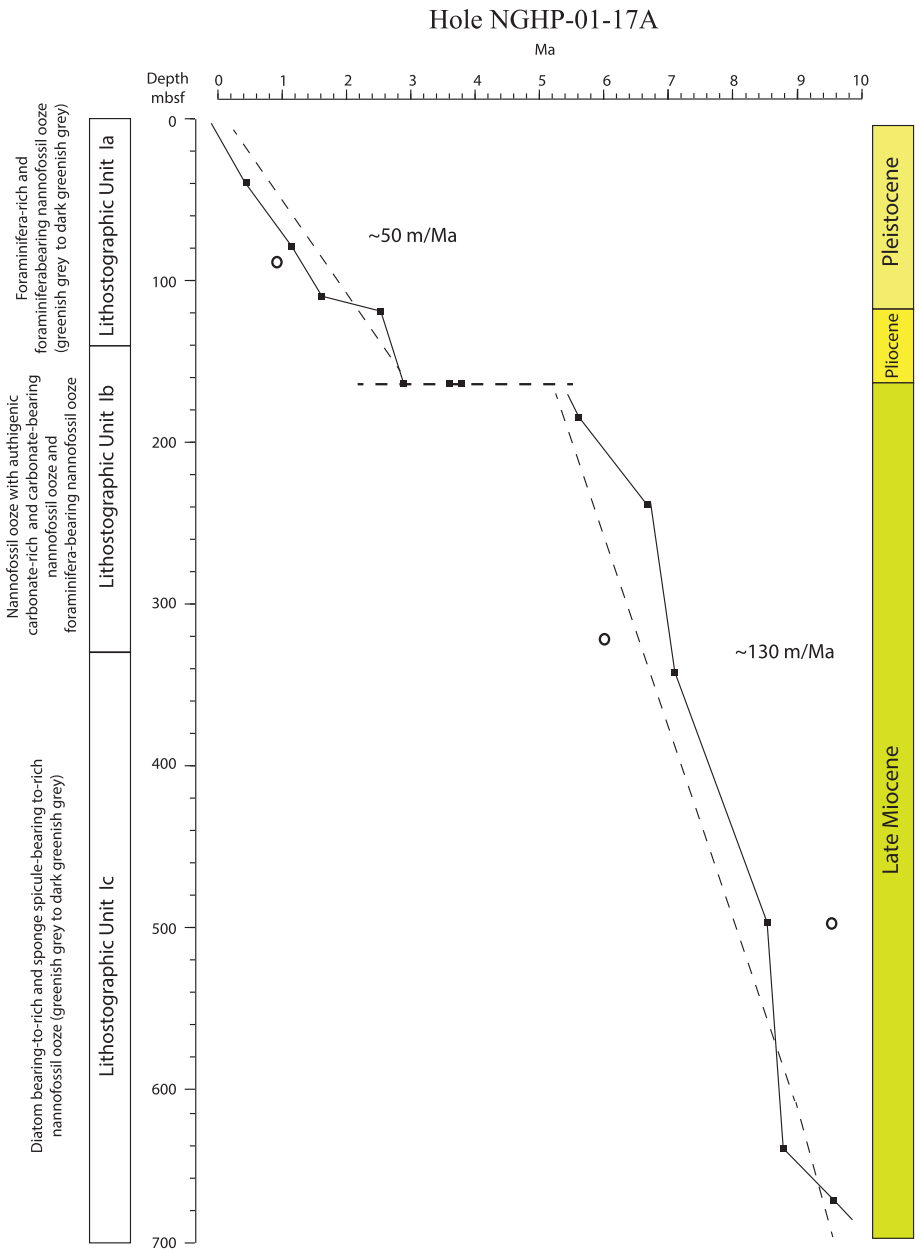

Figure 4. Record of calcareous nannofossil and planktonic foraminifera events vs. age according to ATNTS04 scale for Hole NGHP-01-17A. The circle represents a planktonic foraminifer event (Table 1).

Please cite this article in press as: Flores, J.A., et al., Sedimentation rates from calcareous nannofossil and planktonic foraminifera biostratigraphy in the Andaman Sea, northern Bay of Bengal, and eastern Arabian Sea, Marine and Petroleum Geology (2014), http://dx.doi.org/10.1016/j.marpetgeo.2014.08.011

4.2.1. Pleistocene

Hole NGHP-01-01A was cored to 691 m. The absence of *P. lacunosa* in samples from the core top indicates a late Pleistocene age, younger than 0.46 Myr. Other more recent markers, such as *Emiliania huxleyi* are not present in the samples studied from this record, precluding a better biochronology. Characteristic middle Pleistocene taxa such as *R. asanoi*, are observed. The LO of *R. asanoi* (>6 μm) is placed at 80.72 mbsf; however, above this depth only specimens smaller than 6 μm were observed, thus the HO was not determined. The early Pleistocene is identified by the HO of *C. macintyrei*, that takes place at 109.43 mbsf. The scarcity of discoasters precludes a better biozonal definition. In relation to planktonic foraminifers, the HO of *Globigerinoides fistulosus* is recorded at 99.30 mbsf calibrated at 1.88 Ma (Wade et al., 2011), consistent with the data provided by the calcareous nannofossils. The HO of *G. fistulosus* at 99.30 mbsf marks the end of the Pliocene.

4.2.2. Pliocene

The Pleistocene–Pliocene boundary is approximate here by the HO of *D. surculus* at 118.90 mbsf. Other significant late Pliocene events are well delimited such as the HOs of *D. tamalis*, *Sphenolithus* spp. and the dominance of specimens of *R. pseudoumbilicus* >7 μm. At 165.62 mbsf, both of these are in the same sample, allowing us to interpret a hatius. The next well calibrated event is the HO of *D. quinqueramus* at 185.22 mbsf, approaching the Pliocene–Miocene boundary. The HO of *D. quinqueramus* permits us to approximate duration of about 2.5 Myr for the Pliocene hiatus. The HO of *Neogloboquadrina acostaensis* is recorded at 175.30 mbsf approaching the youngest portion of the early Pliocene, N20 (Kennett and Srinivasan, 1983).

4.2.3. Miocene

Below 185.22 mbsf a characteristic late Miocene assemblage is observed. Circular reticulofenestrids corresponding to *R. rotaria*, were observed upwards 241.59 mbsf. Like in the previous hole, the HO of this species is not well constrained due to the presence of intermediate specimens together with other medium-sized reticulofenestrids. The paracme of *R. pseudoumbilicus* (>7 μm) is defined between 346.50 mbsf (HO) and 644.36 mbsf (LO). In this interval is situated the LO of *D. berggrenii*, at 502.65 mbsf.

The last event is the HO of *D. hamatus*, at 676.85 mbsf, indicating that the bottom of the section is not older than late Miocene. The LO of the planktonic foraminifer *Globorotalia margaritae* is situated at 326.20 mbsf, and the LO of *N. acostaensis* at 496.0 mbsf. Wade et al. (2011) assigned an age of 5.95 Ma and 9.79 Ma to these events, respectively.

4.2.4. Estimation of sedimentation rate

Hole NGHP-01-17A spans the last 10 Ma, with the HO of *D. hamatus* marking the middle Miocene. Three main intervals can be distinguished. From the late Pleistocene to the Pleistocene–-Pliocene boundary (2.5 Ma), at ca. 150 mbsf, the estimated sedimentation rate is around 50 m/Myr. The apparent synchronicity of several events in this horizon is interpreted as a hiatus that covers almost the entire Pliocene. From the Pliocene–Miocene boundary to the base of this hole, the sedimentation rate increases and reaches 130 m/Myr (Fig. 4).

4.3. Hole NGHP-01-19A

Hole NGHP-01-19A was cored to 305 mbsf. This hole shows more restricted calcareous nannofossil information due to the scarcity of markers, as well as a moderate to poor preservation, with intervals sometimes barren in calcareous nannofossils. The distribution of the significant calcareous plankton events is shown in Figure 5 and Table 2.

4.3.1. Pleistocene

Two late Pleistocene to Holocene events are identified: the LO of *E. huxleyi* and the HO of *P. lacunosa*, at 14.98 mbsf and 63.99 mbsf, respectively. Gephyrocapsids and medium sized reticulofenestrid are common, but the species and/or morphotypes observed in other holes, are absent here. Also, although the presence of discoasters in the section is rare, the HO of *Discoaster broweri* is placed at 75.44 mbsf. Alternatively, the absence of *C. macintyrei* prevents a precise assignation of age at this interval because it is not possible the identification of its LO.

4.3.2. Pliocene

The HO of *Sphenolithus* spp. and *R. pseudoumbilicus* are identified at 89.19 mbsf. In this case, however, the lack of significant events, together with a drastic change in the assemblage dominance between *Gephyrocapsa* spp. and *Reticulofenestra* spp. are likely an indication of a hiatus in the record. Its length is difficult to establish due to the absence of references below because of the existing dissolution interval. This dissolved interval, approximately between 100 mbsf and 180 mbsf, covers around 2 Myr (see next section). At 187.13 mbsf the record is constrained by the HO of *D. quinqueramus*, close to the Pliocene–Miocene boundary. The presence of the planktonic foraminifera *Pullentina obliquiloculata* at 43.70 mbsf, confirms a Pliocene age for the lower interval.

4.3.3. Miocene

An assemblage constituted by medium-sized *Reticuloferestra* dominated the lower portion of the core below the dissolved interval. The LO of *D. berggrenii* at 243.89 mbsf marks the late Miocene. Concerning planktonic foraminifers, the LO of *Globorotalia tumida* is identified at 138 mbsf. According to Wade et al. (2011) the age of this event is 5.51 Ma. The LO of *N. acostaensis* is recorded at 213.60 mbsf, at an age of 9.79 Ma. This is coherent with the co-occurrence of *Orbulina universa* at 301.38 mbsf thus assigning the interval a Late Miocene age.

4.3.4. Estimation of sedimentation rate

The scarcity of calcareous nannofossil events due to, both poor preservation (or absence of fossils) and potential ecological limitation of marker species, prevents a precise biochronology, however, estimates of sedimentation rate changes throughout most of the record were obtained and four intervals were differentiated. Sedimentation rates close to 130 m/Myr are estimated for the last 0.5 Ma, while the next interval is characterized by an abrupt drop to values around 10 m/Myr down to the Pleistocene–Pliocene boundary. The occurrence of different biostratigraphic events at 90 mbsf is interpreted as caused by a hiatus in the record, covering the Pliocene. The coincidence of this discontinuity with an interval barren in calcareous nannofossils prevents an accurate estimation of its duration (Fig. 5). The remaining record down to the base of this hole (dated as late Miocene) shows sedimentation rates around 75 m/Myr.

4.4. Hole NGHP-01-18A

Hole NGHP-01-18A was cored to 190 mbsf. The calcareous nannofossil assemblages defined in this hole show a similar distribution to that of Hole NGHP-01-16A, indicating a late Pleistocene age, although with a reduced sedimentation rate. The FO of *E. huxleyi* at 26.83 mbsf indicates an age younger than 0.26 Myr for the materials above this horizon, whereas at 115.91 mbsf, the presence of *P. lacunosa* is consistent with ages older than 0.46 Myr

Please cite this article in press as: Flores, J.A., et al., Sedimentation rates from calcareous nannofossil and planktonic foraminifera biostratigraphy in the Andaman Sea, northern Bay of Bengal, and eastern Arabian Sea, Marine and Petroleum Geology (2014), http://dx.doi.org/10.1016/j.marpetgeo.2014.08.011

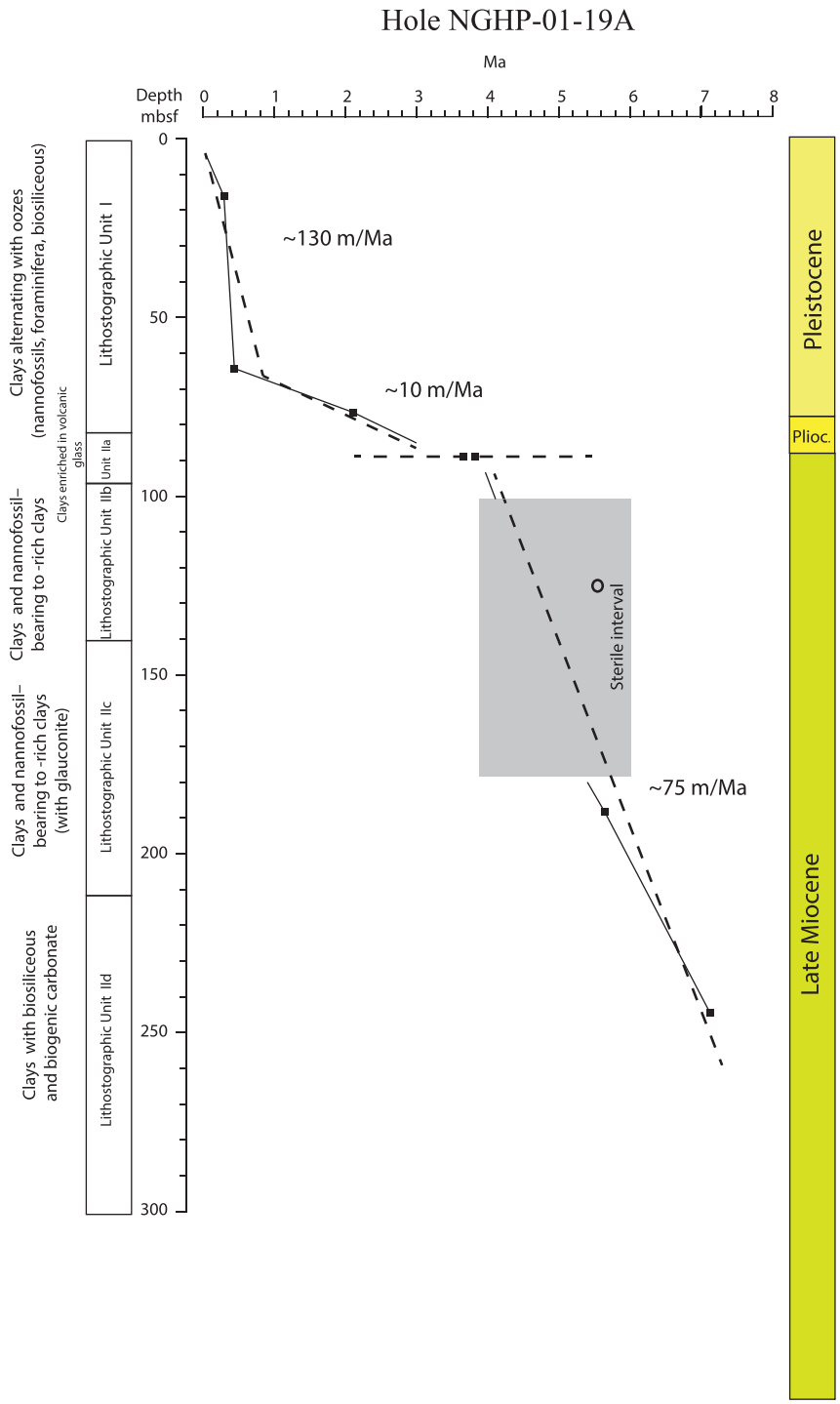

Figure 5. Record of calcareous nannofossil and planktonic foraminifera events vs. age according to ATNTS04 scale for Hole NGHP-01-19A. The small black squares represent calcareous nannofossil events; circles planktonic foraminifers events (Table 1).

below. The distribution of the significant calcareous nannofossils events is shown in Figure 6and Table 2. Planktonic foraminifera biostratigraphy was not attempted at this hole.

4.4.1. Estimation of sedimentation rate

The estimated sedimentation rate for Hole NHGP-01-18A is around 250 m/Myr. In the upper portion of the Late Pleistocene the sedimentation rate is ~135 m/Myr, whereas in the lower portion we estimated sedimentation rates up to 500 m/Myr. The absence of more resolute sampling precludes a more accurate calculation (Fig. 6). Despite the location of Hole NGHP-01-18A in close proximity to Hole NGHP-01-19A, in the Mahanadi basin, it is clear from the calcareous nannofossil biostratigraphy (Table 2 and Figs. 5 and 8) and shipboard site correlation (Collett et al., 2008) that Hole NGHP-01-18A is a younger, expanded section relative to the stratigraphy recovered in Hole NGHP-01-19A.

Please cite this article in press as: Flores, J.A., et al., Sedimentation rates from calcareous nannofossil and planktonic foraminifera biostratigraphy in the Andaman Sea, northern Bay of Bengal, and eastern Arabian Sea, Marine and Petroleum Geology (2014), http://dx.doi.org/10.1016/j.marpetgeo.2014.08.011

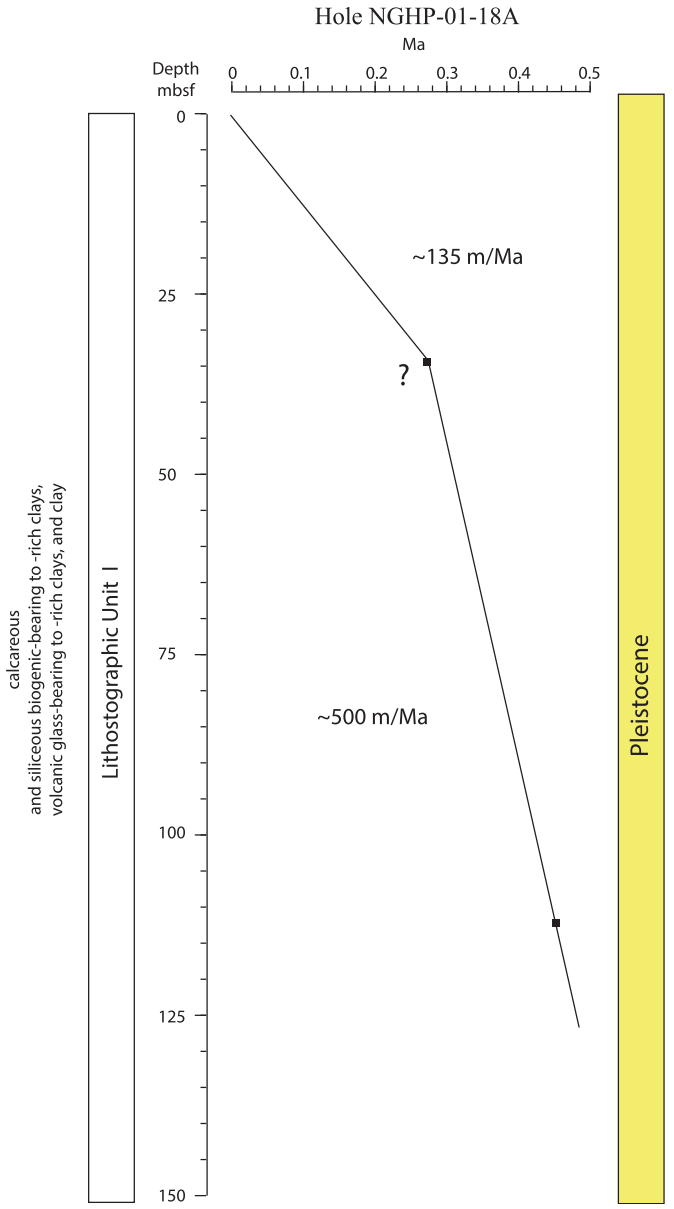

Figure 6. Record of calcareous nannofossil and planktonic foraminifera events vs. age according to ATNTS04 scale for Hole NGHP-01-18A. The small black squares represent calcareous nannofossil events; circles planktonic foraminifers events (Table 1).

4.5. Hole NGHP-01-10B/D

Holes NGHP-01-10B and NGHP-01-10D were cored to 205 and 204 mbsf, respectively. Calcareous nannofossils are scarce in the sediments at this hole. Dissolution is affecting most of the samples analyzed precluding the identification of markers or general features of the assemblage to provide ages. However, the identification of some exemplars of *P. lacunosa* up to 185.83 mbsf, indicates a maximum age of 0.46 Myr at this point. The planktonic foraminifera data available allow us to estimate a Pleistocene–Early Pliocene age. The LO of *Neogloboquadrina dutertrei* is recorded at 179.78 mbsf which indicates the interval 179.78–6.78 mbsf to be Late Pliocene and younger. This is confirmed by the absence of *N. acostaensis* above 186.83 mbsf; its HO is situated near the end of the Pliocene (Kennett and Srinivasan, 1983). Thus, the interval between 186.83 mbsf and 179.78 mbsf represents the latest early Pliocene to mid late Pliocene (Kennett and Srinivasan, 1983). The distribution of the significant calcareous plankton events is shown in Figure 7 and Table 2.

4.5.1. Estimation of sedimentation rate

No precise calcareous plankton events were identified; however, the presence of some Pleistocene taxa allows us to approximate a sedimentation rate around 125 m/Myr (Fig. 7).

4.6. Hole NGHP-01-16A

Hole NGHP-01-16A was cored to 217 mbsf. The calcareous nannofossil assemblage defined at this hole is consistent with a late

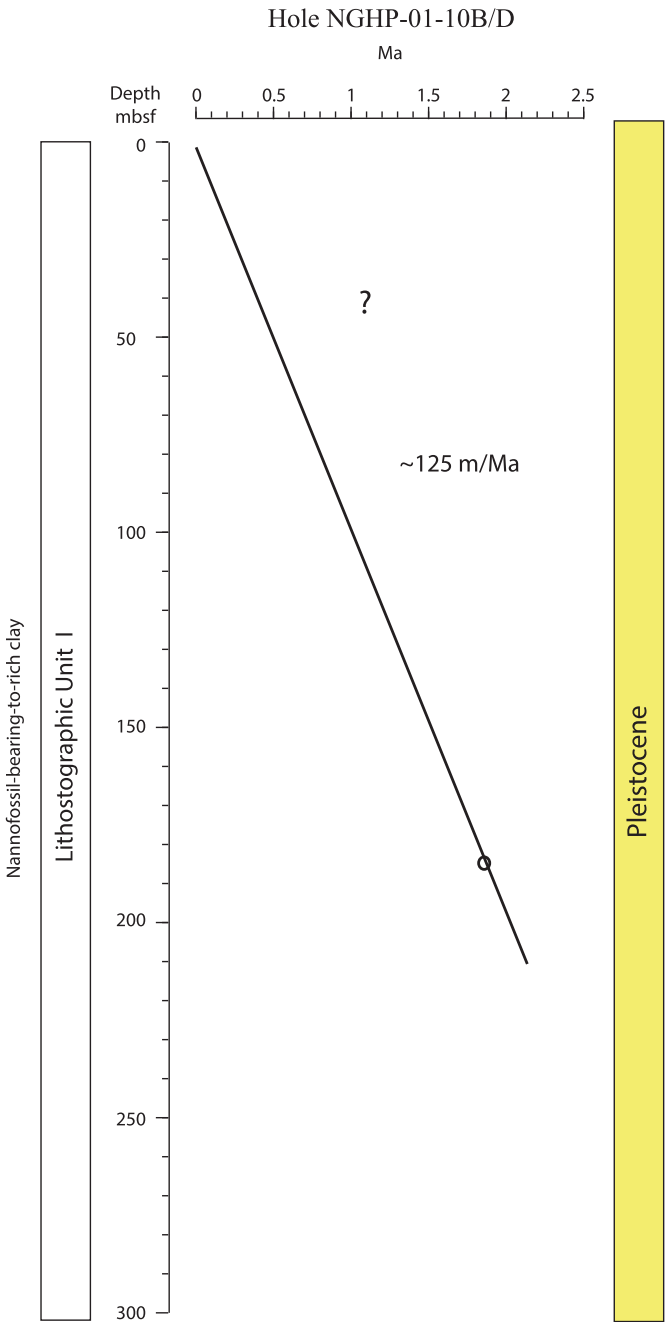

Figure 7. Record of calcareous nannofossil and planktonic foraminifera events vs. age according to ATNTS04 scale for Holes NGHP-01-10B/D.

Please cite this article in press as: Flores, J.A., et al., Sedimentation rates from calcareous nannofossil and planktonic foraminifera biostratigraphy in the Andaman Sea, northern Bay of Bengal, and eastern Arabian Sea, Marine and Petroleum Geology (2014), http://dx.doi.org/10.1016/j.marpetgeo.2014.08.011

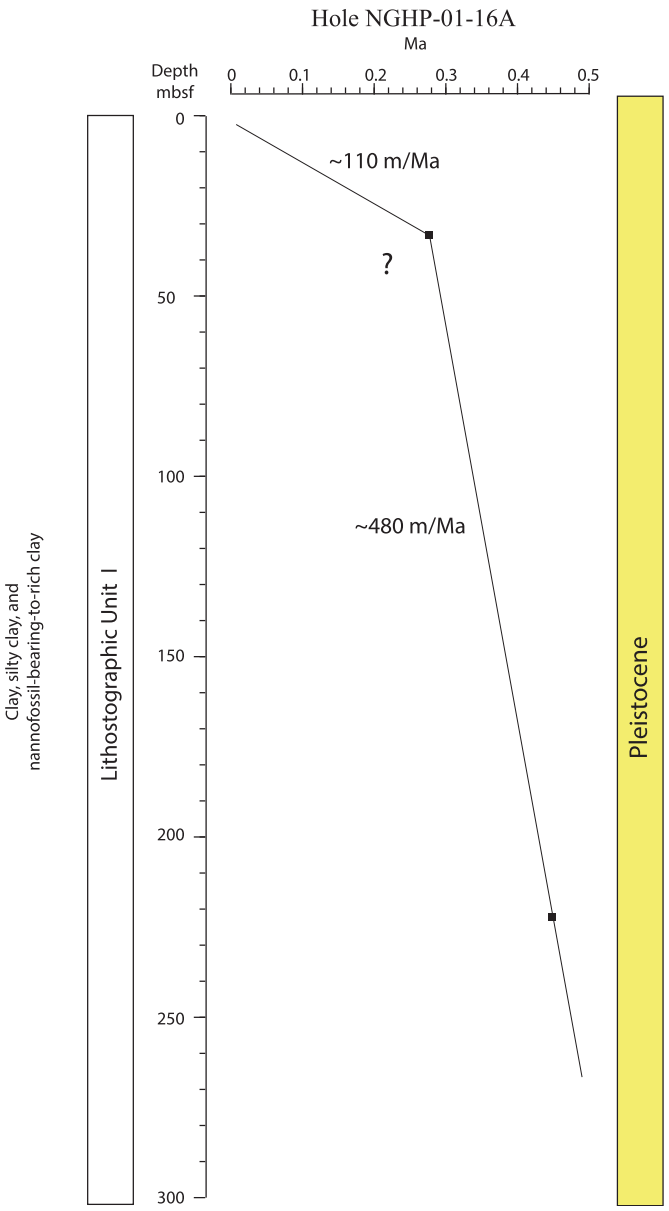

Figure 8. Record of calcareous nannofossil and planktonic foraminifera events vs. age according to AMTS04 scale for Hole NGHP-01-16A. The small black squares represent calcareous nannofossil events (Table 1).

Pleistocene age. The FO of *E. huxleyi* at 31.35 mbsf indicates an age younger than 0.26 Myr above this depth, whereas the presence of *P. lacunosa* at 219.2 mbsf is consistent with ages older than 0.46 Myr below this depth. These data must be taken with caution due to the low resolution of the sampling interval. Figure 8 and Table 2 show the distribution of the significant calcareous nannofossil events. Planktonic foraminifera biostratigraphy was not attempted at this hole.

4.6.1. Estimation of sedimentation rate

The sampling resolution precludes a precise estimation of sedimentation rates. The available calibrated data; however, are consistent with sedimentation rates up to 450 m/Myr, although these values could be lower in the latest portion of the Pleistocene (Fig. 8).

5. Links between sedimentation rate and geological and climate history in the region

The Indian monsoon climate system forms in response to seasonal migration of the intertropical convergence zone (ITCZ) (Gadgil, 2003). The summer monsoon occurs during the northward migration of the ITCZ and the resultant southwesterly winds result in wet, higher precipitation conditions over the Indian region. The winter monsoon occurs during the southward migration of the ITCZ and the resultant northeasterly winds produce drier conditions over the Indian region. The winter and summer monsoons result in drastic changes in surface water salinity, river discharges, surface currents and eddies, and mixed layer depths and stratification, all of which result in changes in the terrigenous sediment fluxes to the continental margins in the flux of biogenic sediments produced through primary and secondary productivity. Changes in the monsoon intensity from decadal to million year timescales have been documented through paleoenvironmental and paleoceanographic proxies applied to many records, including marine sediments (e.g. Clift et al., 2001; Emeis et al., 1995; Oppo and Sun, 2005; Prell et al., 1980; Prell and Kutzbach, 1992, 1997). At Hole NGHP-01-16A Ponton et al. (2012) recently documented extreme drying of India during the late Holocene. Phillips et al., 2014a, reconstruct the last 110 ka of monsoon driven terrestrial and marine sediment fluxes at Hole NGHP-01-19A and document a long interval of enhanced productivity and decreased aridity from 70 to 10 ka. On tectonic timescales, some proxy records suggest an initial intensification of the monsoon occurred at ~7–8 Ma (Kroon et al., 1991; Prell and Kutzbach, 1992), whereas others suggest an earlier intensification at ~22 Ma (Guo et al., 2002; Clift, 2002). It is likely that the longer timescale changes in sedimentation rates documented from the nannofossil and planktonic foraminifera biochronology at these holes reflect large changes in the Indian monsoon system. Significant hiatuses in the Mahanadi basin and Andaman accretionary wedge sites, and dilution or dissolution of calcareous nannofossils in the Krishna–Godavari basin suggest continuous records may not be preserved at Holes NGHP-01-19A and NGHP-01-17A and perhaps siliceous microfossil biostratigraphy could provide a better age model in the K–G basin sites. The sedimentary record at Hole NHGP-01-01A appears continuous through the Oligocene, offering the best location for reconstructing the monsoon over long timescales. The age models developed and the hiatuses identified for these NGHP-01 holes serve as a guide for future biostratigraphic or other age model development along these continental margins and hint at the potential of continental slope sites along the Indian continental margins and in the Andaman accretionary wedge to record long timescale changes in sedimentation influenced by the Indian Monsoon.

6. Conclusions

The identification and placement of calcareous plankton bioevents astronomically calibrated in several holes recovered during the NGHP-01 expedition, allow us to estimate sedimentation rates and hiatuses in sequences containing later Oligocene to Pleistocene age sediments along the Indian continental margin and in the Andaman accretionary wedge. . The western peninsular Indian continental margin shows a continuous Oligocene–Pleistocene sequence with sedimentation rates ranging from 4 to 25 m/Myr. In the Bay of Bengal, both the NW and SE holes recorded a late Miocene–Pleistocene sequence with sedimentation rates of around 45 m/Ma for the Pliocene–Pleistocene, and close to 100 m/Myr for the Miocene. A relevant hiatus is detected both in Holes NGHP-01-17A and NGHP-01-19A, covering most of the Pliocene and late Miocene. In the eastern margin of Peninsular India sedimentation

Please cite this article in press as: Flores, J.A., et al., Sedimentation rates from calcareous nannofossil and planktonic foraminifera biostratigraphy in the Andaman Sea, northern Bay of Bengal, and eastern Arabian Sea, Marine and Petroleum Geology (2014), http://dx.doi.org/10.1016/j.marpetgeo.2014.08.011

rates increase substantially, reaching values from 125 to 500 m/Myr, but extending only to the late Pleistocene.

Acknowledgments

The authors wish to thank those who contributed to the success of the National Gas Hydrate Program Expedition 01 (NGHP-01). NGHP-01 was planned and managed through collaboration between the Directorate General of Hydrocarbons (DGH) under the Ministry of Petroleum and Natural Gas (India), the U.S. Geological Survey (USGS), and the Consortium for Scientific Methane Hydrate Investigations (CSMHI) led by Overseas Drilling Limited (ODL) and FUGRO McClelland Marine Geosciences (FUGRO). The platform for the drilling operation was the research drill ship *JOIDES Resolution*, operated by ODL. Much of the drilling/coring equipment used was provided by the Integrated Ocean Drilling Program (IODP) through a loan agreement with the US National Science Foundation. Wireline pressure coring systems and supporting laboratories were provided by IODP/Texas A&M University (TAMU), FUGRO, USGS, U.S. Department of Energy (USDOE) and HYACINTH/GeoTek. Downhole logging operational and technical support was provided by Lamont-Doherty Earth Observatory (LDEO) of Columbia University. The financial support for the NGHP01, from the Oil Industry Development Board, Oil and Natural Gas Corporation Ltd., GAIL (India) Ltd. and Oil India Ltd. is gratefully acknowledged. We also acknowledge the support extended by all the participating organizations of the NGHP: MoP&NG, DGH, ONGC, GAIL, OIL, NIO, NIOT, and RIL. This research was also supported by the Ministerio de Economía y Competitividad PASUR CGL2009-08651 and VACLIODP339 CTM2012-38248 projects and the U.S. Geological Survey (Contract # 07CRSA0708).

References

Babu, C.P., Pattan, J.N., Dutta, K., Basavaiah, N., Ravi Prasad, G.V., Ray, D.K., Govil, P., 2010. Shift in detrital sedimentation in the eastern Bay of Bengal during the late Quaternary. J. Earth Syst. Sci. 119, 285–295.

Bastia, R., Das, S., Radhakrishna, M., 2010. Pre- and post-collisional depositional history in the upper and middle Bengal fan and evaluation of deepwater reservoir potential along the northeast continental margin of India. Mar. Pet. Geol. 27, 2051–2061.

Blow, W.H., 1969. Late middle Eocene to recent planktonic foraminiferal biostratigraphy. In: Bronnimann, P., Renz, H.H. (Eds.), Proceedings of the First International Conference on Planktonic Microfossils, Geneva 1967, vol. 1, pp. 199–422.

Bowles, F., Ruddiman, W., Jahn, W., 1978. Acoustic stratigraphy, structure, and depositional history of the Nicobar Fan, Eastern Indian Ocean. Mar. Geol. 26, 269–288.

Backman, J., Shackleton, N.J., 1983. Quantitative biochronology of Pliocene and Early Pleistocene calcareous nannofossils from the Atlantic, Indian and Pacific oceans. Mar. Micropaleontol. 8, 141–170.

Berggren, W.A., Kent, D.V., Swisher III, C.C., Aubry, M., 1995. A revised Cenozoic geochronology and chronostratigraphy. In: Berggren, W.A., et al. (Eds.), Geochronology, Time Scales and Global Stratigraphic Correlation, 54. SEPM Special Publication, pp. 129–212.

Bown, P.R., Young, J.R., 1998. In: Bown, P.R. (Ed.), Calcareous Nannofossil Biostratigraphy. Chapman & Hall, Londres, p. 314.

Bukry, D., 1991. Paleoecological Transect of Western Pacific Ocean Late Pliocene Coccolith Flora, Part I. Tropical Ontong-Java Plateau at ODP 806B. Open-File Rep. US Geol. Surv. 91-552, pp. 1–35.

Campanile, D., Nambiar, C.G., Bishop, P., Widdowson, M., Brown, R., 2008. Sedimentation record in the Konkan-Kerala Basin: implications for the evolution of the Western Ghats and the Western Indian passive margin. Basin Res. 20, 3–22.

Cawthern, T., Johnson, J.E., Giosan, L., Flores, J.A., Rose, K., Solomon, E., 2014. A Late Miocene-Early Pliocene Biogenic Silica Crash in the Andaman Sea and Bay of Bengal: potential teleconnections to the Pacific. J. Mar. Pet. Geol. SI India Gas Hydrates (in press).

Chakrapani, G.J., Subramanian, V., 1990. Preliminary studies on the geochemistry of the Mahanadi River basin, India. Chem. Geol. 81, 241–253. http://dx.doi.org/10.1016/0009-2541(90)90118-Q.

Clift, P.D., Shimiz, N., Layne, G.D., Blusztajn, J.S., Gaedicke, C., Schlüter, H.-U., Clark, M.K., Amjad, S., 2001. Development of the Indus Fan and its significance for the erosional history of the Western Himalaya and Karakoram. Geol. Soc. Am. Bull. 113, 1039–1051.

Clift, P.D., 2002. A brief history of the Indus River. In: Clift, P., Kroon, D., Gaedicke, C., Craig, J. (Eds.), Tectonic and Climatic Evolution of the Arabian Sea Region, Geological Society London, Special Publication, 195, pp. 97–116.

Collett, T.S., Riedel, M., Cochran, J.R., Boswell, R., Presley, J., Kumar, P., Sathe, A., Sethi, A., Lall, M., Sibal, V., NGHP Expedition 01 Scientists, 2008. National Gas Hydrate Program Expedition 01 Initial Reports. Directorate General of Hydrocarbons, New Delhi.

Curray, J.R., Emmel, F.J., Moore, D.G., 2003. The Bengal Fan: morphology, geometry, stratigraphy, history and processes. J. Mar. Pet. Geol. 19, 1191–1223.

De Kaenel, E., Villa, G., 1996. Oligocene-Miocene Calcareous Nannofossil Biostratigraphy and Paleoecology from the Iberia Abyssal Plain. Proc. ODP Sci. Results 149, 79–145.

Duncan, R.A., Pyle, D.G., 1988. Rapid eruption of the Deccan flood basalts at the Cretaceous/Tertiary boundary. Nature 333, 841–843.

Emeis, K.-C., Anderson, D.M., Doose, H., Kroon, D., Schulz-Bull, D., 1995. Sea-surface temperatures and the history of monsoon upwelling in the northwest Arabian Sea during the last 500,000 years. Quat. Res. 43, 355–361.

Fisk, M.R., Duncan, R.A., Baxter, A.N., Greenough, J.D., Hargraves, R.B., Tatsumi, Y., 1989. Reunion hotspot magma chemistry over the past 65 m.y.: results from Leg 115 of the Ocean Drilling Program. Geology 17, 934–937.

Flores, J.A., Marino, M., 2002. Pleistocene calcareous nannofossil stratigraphy for ODP Leg 177 (Atlantic sector from the Southern Ocean). Mar. Micropaleontol. 45, 1–34.

Fornaciari, E., Rio, D., 1996. Latest Oligocene to early middle Miocene quantitative calcareous nannofossil biostratigraphy in the Mediterranean region. Micropaleontology 42, 1–36.

Fornaciari, E., Raffi, I., Rio, D., Villa, G., Backman, J., Olafsson, G., 1990. Quantitative Distribution Pattern of Oligocene and Miocene Calcareous Nannofossils from Western Equatorial Indian Ocean. Proc. ODP Sci. Results 115, 237–254.

Fornaciari, E., Backman, J., Rio, D., 1993. Quantitative Distribution Patterns of Selected Lower to Middle Miocene Calcareous Nannofossils from the Ontong Java Plateau. Proc. ODP Sci. Results 130, pp. 245–256.

Fornaciari, E., Di Stefano, A., Rio, D., Negri, A., 1996. Middle Miocene quantitative calcareous nannofossil biostratigraphy in the Mediterranean region. Micropaleontology 42, 37–63.

Gadgil, S., 2003. The Indian Monsoon and its variability. Annu. Rev. Earth Planet. Sci. 31, 429–467.

Gartner, S., 1992. Miocene nannofossil chronology in the North Atlantic DSDP site 608. Mar. Micropaleontol. 18, 307–331.

Gradstein, F.M., Ogg, J.G., Smith, A.G., 2004. A Geologic Time Scale 2004. Cambridge University Press, p. 589.

Guo, Z.T., Ruddiman, W.F., Hao, Q.Z., Wu, H.B., Qiao, Y.S., Zhu, R.X., Peng, S.Z., Wei, J.J., Yuan, B.Y., Liu, T.S., 2002. Onset of Asian desertification by 22 Myr ago inferred from loess deposits in China. Nature 416, 159–163.

Johnson, J.E., Phillips, S.C., Torres, M.E., Pinero, E., Rose, K.K., Giosan, L., 2014. Influence of total organic carbon deposition on the inventory of gas hydrate in the Indian continental margins. J. Mar. Pet. Geol. SI India Gas Hydrates (in press).

Kalaswad, S., et al., 1993. Evolution of the continental-margin of western India – new evidence from apatite fission-track dating. J. Geol. 101, 667–673.

Karig, D.E., Lawrence, M., Moore, G., Curray, J., 1980. Structural framework of the fore-arc basin, NW Sumatra. J. Geol. Soc. Lond. 137, 77–91.

Kennett, J.P., Srinivasan, M.S., 1983. Neogene Foraminifera: a Phylogenetic Atlas. Hutchinson Ross Publishing Company, Stroudsburg, PA, 265 pp.

Kroon, D., Steens, T.N.F., Troelstra, S.R., 1991. Onset of monsoonal related upwelling in the western Arabian Sea as revealed by plankonic foraminifers. In: Prell, W.L., Niitsuma, N., Emeis, K.C., Meyers, P. (Eds.), Proc. ODP Sci. Results, 117, pp. 257–264.

Lourens, L.J., Hilgen, F.J., Shackleton, N.J., Laskar, J., Wilson, D., 2004. The Neogene period. In: Gradstein, F.M., Ogg, J.G., Smith, A.G. (Eds.), A Geological Time Scale 2004. Cambridge University Press, Cambridge, pp. 409–440.

Maiorano, P., Monechi, S., 1998. Revised correlation of Early and Middle Miocene calcareous nannofossil events and magnetostratigraphy from DSDP site 563 (North Atlantic Ocean). Mar. Micropaleontol. 35, 235–255.

Marino, M., Flores, J.A., 2002a. Miocene to Pliocene Calcareous nannofossil biostratigraphy at ODP Leg 177 sites 1088 and 1090. Mar. Micropaleontol. 45, 291–307.

Marino, M., Flores, J.A., 2002b. Middle Eocene to Early Oligocene calcareous nannofossils and biomagnetostratigraphy at Leg 177 site 1090. Mar. Micropaleontol. 45, 383–398.

Martini, E., 1971. Standard Tertiary and Quaternary calcareous nannoplankton zonation. In: Farinacci, A. (Ed.), Proceedings of the II Planktonic Conference, 2. Ed. Tecnoscienza, Roma, pp. 739–785, 1970.

Okada, H., Bukry, D., 1980. Supplementary modification and introduction of code numbers to the low-latitude coccolith biostratigraphic zonation (Bukry, 1973; 1975). Mar. Micropaleontol. 5, 321–325.

Olafsson, G., 1989. Quantitative Calcareous Nannofossil Biostratigraphy of Upper Oligocene to Middle Miocene Sediments from ODP Hole 667A and Middle Miocene Sediments from DSDP Site 754. Proc. ODP Sci. Results 108, 9–22.

Oppo, D.W., Sun, Y., 2005. Amplitude and timing of sea surface temperature change in the northern South China Sea: dynamic link to the East Asian Monsoon. Geology 33, 785–788.

Pal, T., Chakraborty, P., Gupta, T., Singh, C., 2003. Geodynamic evolution of the outer-arc—forearc belt in the Andaman Islands, the central part of the Burma-Java subduction complex. Geol. Mag. 140, 289–307.

Please cite this article in press as: Flores, J.A., et al., Sedimentation rates from calcareous nannofossil and planktonic foraminifera biostratigraphy in the Andaman Sea, northern Bay of Bengal, and eastern Arabian Sea, Marine and Petroleum Geology (2014), http://dx.doi.org/10.1016/j.marpetgeo.2014.08.011

Perch-Nielsen, K., 1985. Cenozoic calcareous nannofossils. In: Bolli, H.M., Saunders, J.B., Perch-Nielsen, K. (Eds.), Plankton Stratigraphy. Cambridge University Press, Cambridge, pp. 427–554.

Phillips, S.C., Johnson, J.E., Giosan, L., Rose, K., 2014a. Monsoon-influenced variation in productivity and lithogenic sediment flux since 110 ka in the offshore Mahanadi Basin, northern Bay of Bengal. J. Mar. Pet. Geol. SI India Gas Hydrates (in press).

Phillips, S.C., Johnson, J.E., Guo, J., Underwood, M.B., Hahn, J., Rose, K., Giosan, L., 2014b. Bulk and clay mineral composition of sediments of the Bay of Bengal, Andaman Sea, and Arabian Sea recovered during NGHP Expedition 01. J. Mar. Pet. Geol. SI India Gas Hydrates (in press).

Ponton, C., Giosan, L., Eglinton, T.I., Fuller, D.Q., Johnson, J.E., Kumar, P., Collett, T.S., 2012. Holocene aridification of India. Geophys. Res. Lett. 39 (L03704) http://dx.doi.org/10.1029/2011GL050722.

Powell, C.M., Roots, S.R., Veevers, J.J., 1988. Pre-breakup continental extension in East Gondwanaland and the early opening of the eastern Indian Ocean. Tectonophysics 155, 261–283.

Prell, W.L., Hutson, W.H., Williams, D.F., Be, A.W.H., Geitnenauer, K., Molfino, B., 1980. Surface circulation of the Indian Ocean during the Last Glacial Maximum, approximately 18,000 yr B.P. Quat. Res. 14, 309–336.

Prell, W.L., Kutzbach, J.E., 1992. Sensitivity of the Indian monsoon to forcing parameters and implications for its evolution. Nature 360, 647–653.

Prell, W.L., Kutzbach, J.E., 1997. The impact of Tibetan–Himalayan elevation on the sensitivity of the monsoon climate system to changes in solar radiation. In: Ruddiman, W.F. (Ed.), Tectonic Uplift and Climate Change. Plenum Press, New York, pp. 171–201.

Radhakrishna, M., Twinkle, D., Nayak, S., Bastia, R., Rao, G.S., 2012. Crustal structure and rift architecture across the Krishna-Godavari Basin in the central Eastern Continental Margin of India based on analysis of gravity and seismic data. J. Mar. Pet. Geol. 37, 129–146.

Raffi, I., Flores, J.A., 1995. Pleistocene Through Miocene Calcareous Nannofossils from Eastern Equatorial Pacific Ocean (Leg 138). Proc. ODP Sci. Results 138, 233–282.

Raffi, I., Rio, D., d'Atri, A., Fornaciari, E., Rocchetti, S., 1995. Quantitative Distribution Patterns and Biomagnetostratigraphy of Middle and Late Miocene Calcareous Nannofossils from Equatorial Indian and Pacific Oceans (Leg 115, 130, and 138). Proc. ODP Sci. Results 138, 479–502.

Raffi, I., Backman, J., Fornaciari, E., Pälike, H., Rio, D., Lourens, L., Hilgen, F.J., 2006. A review of calcareous nannofossil astrobiochronology encompassing the past 25 million years. Quat. Sci. Rev. 25, 3113–3137.

Raju, K.A., Murty, G., Amarnath, D., Kumar, M., 2007. The west Andaman fault and its influence on the aftershock pattern of the recent megathrust earthquakes in the Andaman-Sumatra region. Geophys. Res. Lett. 34, 1–5.

Ramana, M.V., Ramprasad, T., Desa, M., 2001. Seafloor spreading magnetic anomalies in the Enderby basin, East Antarctica. Earth Planet. Sci. Lett. 191, 241–255.

Ramaswamy, V., Nair, R.R., Manganini, S., Haake, B., Ittekkot, V., 1991. Lithogenic fluxes to the deep Arabian Sea measured by sediment traps. Deep-Sea Res. 38, 169–184.

Ramaswamy, V., Gaye, B., Shirodkar, P.V., Rao, P.S., Chivas, A.R., Wheeler, D., Thwin, S., 2008. Distribution and sources of organic carbon, nitrogen and their isotopic signatures in sediments from the Ayeyarwady (Irrawaddy) continental shelf, northern Andaman Sea. Mar. Chem. 111, 137–150.

Rickers, K., Mezger, K., Raith, M.M., 2001. Evolution of the continental crust in the Proterozoic Eastern Ghats Belt, India and new constraints for Rodinia reconstruction: implications from Sm-Nd, Rb-Sr and Pb-Pb isotopes. Precambrian Res. 112, 183–210.

Rio, D., Fornaciari, E., Raffi, I., 1990a. Late Oligocene Through Early Pleistocene Calcareous Nannofossils from Western Equatorial Indian Ocean (Leg 115). Proc. ODP Sci. Results 115, 175–221.

Rio, D., Raffi, I., Villa, G., 1990b. Pliocene-Pleistocene Calcareous Nannofossil Distribution Patterns in the Western Mediterranean. Proc. ODP Sci. Results 107, 513–533.

Rodolfo, K., 1969. Bathymetry and marine geology of the Andaman Basin, and tectonic implications for Southeast Asia. Geol. Soc. Am. Bull. 80, 1203–1230.

Rodolfo, K.S., 1975. The Irrawaddy Delta: Tertiary setting and modern offshore sedimentation. In: Broussard, M.L. (Ed.), Deltas: Models for Exploration. Houston Geological Society, Houston, pp. 329–348.

Rose, K., Johnson, J.E., Torres, M., Hong, W., Giosan, L., Solomon, E., Kastner, M., Cawthern, T., Long, P., Schaef, H., 2014. Preferential accumulation of gas hydrate in porous-permeable volcanic ash beds of the Andaman Arc, NGHP-01 site 17. J. Mar. Pet. Geol. SI India Gas Hydrates (in press).

Royer, J.Y., Chaubey, A.K., Dyment, J., Bhattacharya, G.C., Srinivas, K., Yatheesh, V., Ramprasad, T., 2002. Paleogene plate tectonic evolution of the Arabian and Eastern Somali basins. In: Clift, P., et al. (Eds.), The Tectonic and Climatic Evolution of the Arabian Sea Region. Geological Society, London, pp. 7–23.

Sato, T., Takayama, T., 1992. A stratigraphical significant new species of the calcareous nannofossil *Reticulofenestra asanoi*. In: Ishizaki, K., Saito, T. (Eds.), Centenary of Japanese Micropaleontology. Terra Scientific, Tokyo, pp. 457–460.

Subramanian, V., 1980. Mineralogical input of suspended matter by Indian rivers into the adjacent areas of the Indian Ocean. Mar. Geol. 36, 29–34.

Tripathy, G.R., Singh, S.K., Bhushan, R., Ramaswamy, V., 2011. Sr-Nd isotope composition of the Bay of Bengal sediments: impact of climate on erosion in the Himalaya. Geochemical Journal 45, 175–186.

Wade, B.S., Pearson, P.N., Berggren, W.A., Paelike, H., 2011. Review and revision of Cenozoic tropical planktonic foraminiferal biostratigraphy and calibration to the geomagnetic polarity and astronomical time scale. Earth Sci. Rev. 104, 111–142.

Please cite this article in press as: Flores, J.A., et al., Sedimentation rates from calcareous nannofossil and planktonic foraminifera biostratigraphy in the Andaman Sea, northern Bay of Bengal, and eastern Arabian Sea, Marine and Petroleum Geology (2014), http://dx.doi.org/10.1016/j.marpetgeo.2014.08.011